JOURNAL OF PROPULSION AND POWER
Vol. 15, No. 6, November–December 1999

Flame Propagation Processes in a Simulated Combustor for Heated-Gas Airbag Inflators

Grant A. Risha,* Kenneth K. Kuo,† Yeu-Cherng Lu,‡ and Donald E. Koch§
Pennsylvania State University, University Park, Pennsylvania 16802
and
Harold Blomquist¶ and Abdel K. Helmy**
TRW-Vehicle Safety Systems, Inc., Mesa, Arizona 85215

An experimental investigation was conducted to study the flame propagation processes of premixed hydrogen/air flames in a test rig simulating conditions in heated-gas inflators for the advancement of the hybrid airbag device. The major objective was to observe the coupling phenomena of the igniter discharge and flame propagation process under different test conditions. Using high-speed cinematography, the flame-front propagation speed was found to be governed by the trajectory of the ejected igniter disk. Initial concentration of hydrogen has a dominant effect on the pressure–time history in the combustor. It was found that, for marginally lean mixtures, the occurrence of the nonreproducible feature of the second pressure hump, during the chamber depressurization process, was caused by the strong coupling between the igniter disk trajectory and the wake-flow induced reactions of entrained gases.

Introduction

OVER the past 30 years, a wide range of gas generator technologies have been explored to meet the demands of motor vehicle airbag applications.[1] When the National Highway Traffic Safety Association mandated passive restraint technology with "Standard 208; Occupant crash protection," the production base responded with prevailing airbag designs pioneered from the mid-1960s through the 1980s, primarily with those based on sodium azide/metal oxide combustion. Key benefits of these systems include low combustion temperature, nontoxic effluent combustion products, high propellant burning rate, and simple designs inasmuch as high-pressure gas storage is not required. Drawbacks to this approach include the toxicity of azide mixtures (which are supplied in hermetically sealed containers) and cost when compared to other alternatives to be discussed. Other airbag inflator designs were also developed[2] wherein high-pressure stored gas was heated by supplying the stored gas with propellant combustion products released inside the pressure vessel. Manufacturing processes have evolved that demonstrate high reliability for sealing the high-pressure gas compartment. Key advantages include 10-fold reduction in solid-propellant mass, use of less toxic propellant ingredients, and reduced costs. In spite of these advantages, issues still exist concerning effluent combustion products and noticeable levels of smoke. A new TRW technology, referred to as the heated-gas inflator (HGI), has emerged that heats the stored gas by combusting a portion of mixture itself, thus eliminating the solid propellant altogether.[3]

An example mixture is hydrogen/oxygen/nitrogen, wherein the reactive gases are ignited inside the high-pressure storage vessel providing heat to create, for deployment purposes, more efficient use of the stored gas present. Key advantages are simplicity, reduced ingredient toxicity, improved combustion byproducts (water vapor), tailorable performance, high reproducibility, and low cost.[4] Other inflator designs are described in Refs. 5 and 6. The disadvantages of the conventional solid-propellant airbags are discussed in Refs. 7 and 8.

This study was designed to provide pressure, temperature, and geometric details of the combustion process resolved both temporally and spatially. The motivation of this basic research is to provide improved understanding of physical processes for improved tailorability of the system design and insight into the initiation and propagation of the flame front within the pressure vessel at different initial pressures. The experimental results also can serve to validate computer model simulation of the system function.

To simulate the HGI processes the combustion chamber was charged with gaseous hydrogen and air and was ignited using TRW designed pyrotechnic initiators mounted in the assembly. This assembly also controls the discharge feature of the burned gas through an annular passage. Upon ignition, combustion of premixed gases causes the chamber pressure to build up. A portion of the burned gas begins to discharge from the combustor and inflate the airbag. During the flow discharge process, combustion of premixed gases continues inside of the chamber.

Objectives

The primary objective of this study is to improve the fundamental understanding of the combustion processes using a windowed high-pressure combustion chamber and a high-speed movie camera. Simultaneous pressure and temperature measurements allow interpretation of the gasdynamics aspects of these observations.

Four specific objectives for high-speed cinematography were identified: 1) to visualize the igniter discharge event, 2) to observe the ignition process of the premixed H_2/air mixture by the igniter jet, 3) to deduce the flame-front propagation rate, and 4) to study the dynamic behavior of the flame during the ballistic cycle.

For the four observable events just enumerated, the experimental variables of interest were as follows: 1) to investigate the effects of initial chamber pressure, 2) to determine the effect of gas composition, and 3) to develop a diagnostic method to observe spatial and temporal variations in a nonluminous flame structure utilizing a pulsed copper-vapor laser sheet.

Four specific objectives for transient temperature and pressure measurements were identified: 1) to obtain the gas temperature–time variations at several locations within the chamber, 2) to measure

Received 16 July 1998; revision received 18 March 1999; accepted for publication 29 March 1999. Copyright © 1999 by the American Institute of Aeronautics and Astronautics, Inc. All rights reserved.

*Graduate Student, Department of Mechanical and Nuclear Engineering. Member AIAA.
†Distinguished Professor and Director of the High Pressure Combustion Laboratory, Department of Mechanical and Nuclear Engineering. AIAA Fellow.
‡Research Associate, Department of Mechanical and Nuclear Engineering; currently Engineer, P.O. Box 97009, Primex Aerospace Company, 11441 Willows Road N.E., Redmond, WA 98073-9709. Member AIAA.
§Research Assistant, Department of Mechanical and Nuclear Engineering.
¶Manager, Propellant and Combustion Research and Development.
**Senior Staff Engineer.

the bulk gas temperature in the exhaust port to verify that the gas temperature is suitable for an airbag application, 3) to obtain the pressurization rate in the chamber, and 4) to study the pressure–time history of the transient event.

Method of Approach

Experimental Setup

The combustion experiments were conducted in a high-pressure stainless steel windowed chamber, as shown in Fig. 1. The chamber has an inner diameter of 7.6 cm (3 in.) and is capable of sustaining pressures up to 68.9 MPa (10,000 psi). The volume of the chamber is approximately 1041 ml. The chamber consists of four Plexiglas® window ports, located 90 deg apart. The viewing port of each window is 95 × 31.8 mm (3.75 × 1.25 in.). A top view of the experimental setup and optical data acquisition system is shown in Fig. 2.

Three ports were fitted with Plexiglas windows. One port served as an optical viewing window for recording the flame-spreading and combustion events by a high-speed movie camera (HYCAM) and/or a charge-coupled device (CCD) video camera. Two other ports, perpendicular to the observation port, provide entrance and exit for the copper-vapor laser sheet, which enhanced temporal resolution and provided illumination of combustion products forming in the flame front. A copper-vapor laser sheet that was optically transformed from a cylindrical laser beam was aligned to pass through these two windows for laser-illuminated flow visualization and high-speed cinematography. The fourth port was fitted with a steel plate on which three pressure transducers and two fine-wire thermocouples were mounted through their respective ports.

The TRW igniter was mated to the high-pressure windowed chamber by fabricating a reusable end plate housing from 304 stainless steel, shown in Fig. 3. This element positioned the igniter discharge

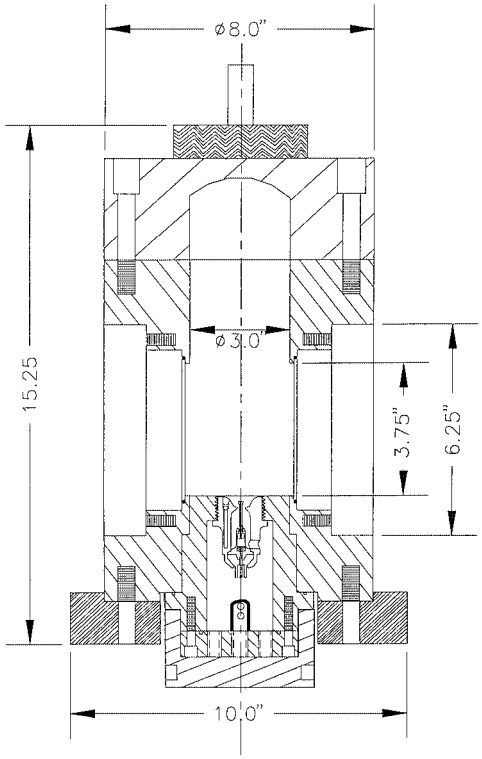

Fig. 1 Assembly drawing of high-pressure combustion chamber.

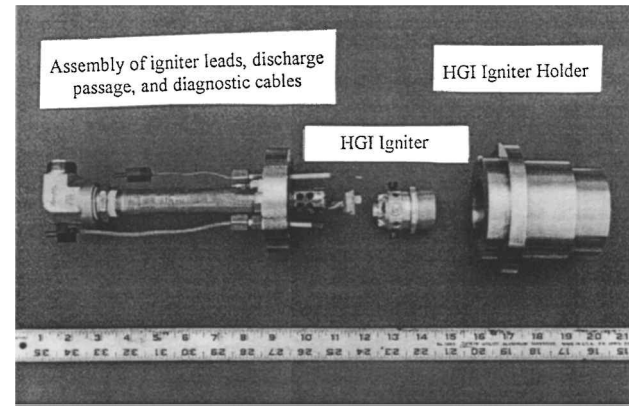

Fig. 3 Photograph of the exploded view of the HGI igniter housing and base plate.

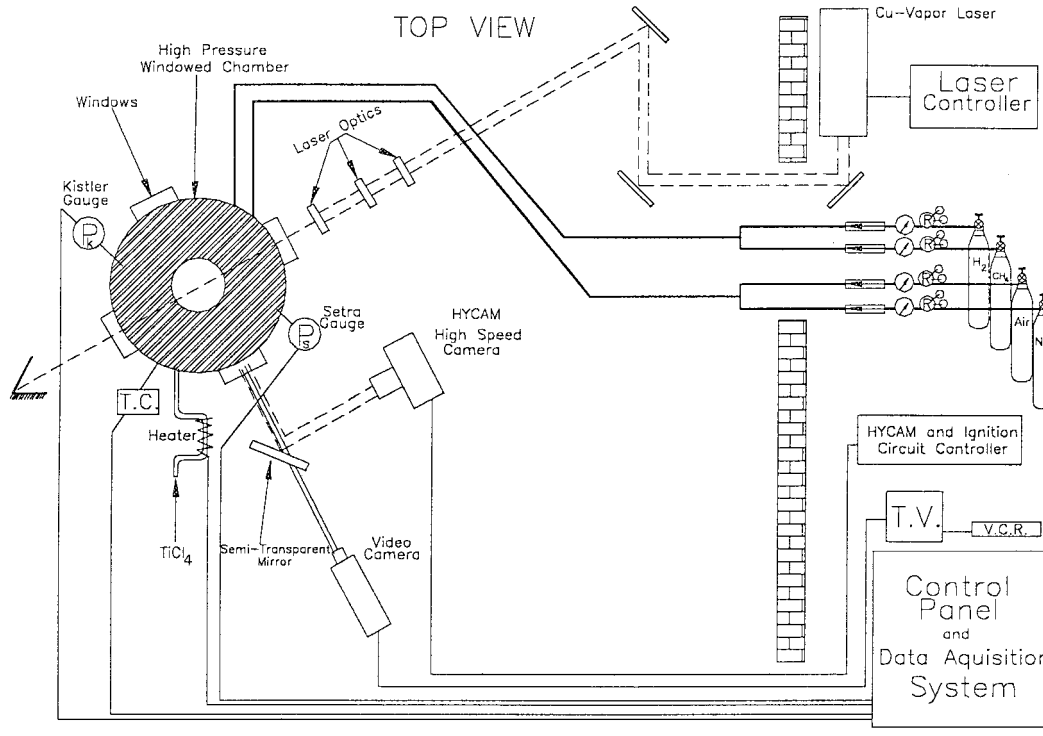

Fig. 2 Top view of the experimental setup and optical data acquisition system.

in the viewing area, housed the feed through for the igniter circuit wires, provided a discharge passage for the exiting hot gas flow, and sealed the high-pressure vessel prior to ignition. The top portion of the igniter detaches upon ignition; the ejected disk travels into premixed gases in the vessel. The TRW igniter was sealed in the housing using a 4.8 mm ($\frac{3}{16}$ in.) O-ring.

On the exhaust side of the end plate, a dome-shaped vented cover was placed at the exhaust port entrance to restrain the motion of the igniter leads within the igniter holder cavity to extend the lifetime of the igniter lead wire/connector. The igniter leads were each used for approximately five test runs before they were discarded. The dome-shaped porous cover was designed to protrude above the exhaust port entrance also to prevent the possibility of the igniter leads lodging into the exhaust port for flow blockage. The base plate of the igniter holder consisted of an exhaust gas port and several diagnostic ports for thermocouple and pressure transducer measurements for monitoring the exhaust port conditions. Note that the observed combustion processes in the combustor were not affected by the downstream exhaust conditions due to the choked flow condition in the HGI igniter assembly. In the present investigation, the gases were exhausted to the atmospheric pressure instead of a 146-liter discharge tank. Again, the chamber processes are not affected because the exhaust flow was choked at the annular restriction station of the HGI igniter.

Instrumentation

Figure 2 is a schematic diagram showing the optical diagnostic setup, data acquisition system, and gas feedlines. Several fine-wire thermocouples were used to measure the temperatures of the burned gas and the exhaust gas. These S-type thermocouples were constructed at the Pennsylvania State University laboratory by welding 25-μm pure platinum wire to an alloy wire containing 10% rhodium and 90% platinum. To measure the burned-gas temperature, two thermocouples were placed approximately 5 cm apart in the diagnostic window replacement plate with intrusion distances of 6 and 25 mm from the chamber wall, respectively. For the measurement of the exhaust gas temperature, two thermocouples were installed in the annular space in the base plate of the HGI igniter holder (see Fig. 1).

Five fast-response pressure transducers (Kistler 601B1) were used to measure the pressure–time history during the test run. Three of the pressure transducers were installed in the diagnostic window replacement plate spaced 35.6 mm (1.4 in.) apart and two pressure transducers were installed in the base plate to record exhaust gas conditions. Two thermocouples were also installed in the diagnostic window replacement plate spaced 35.6 mm (1.4 in.) apart. Both the thermocouple and the pressure transducer outputs were measured in voltages. These voltages were recorded by a multichannel Nicolet data acquisition system and displayed in millivolts. To obtain actual pressure measurements from the recorded data, a linear calibration plot was employed.

Gas Mixing and Filling Procedure

Ultra-high-purity gases were used in this study. For air, the purity level was classified as ultrazero, and the purity level of the hydrogen was 99.999%. The specific concentrations were listed in molar form. Therefore, desired mixtures were obtained by filling the vessel to the appropriate partial pressure of each gas component. Because the partial pressures were determined using the ideal gas law, a high-pressure effect was considered. For the pressure range considered in this investigation, the results of the ideal gas law were compared to the Beattie–Bridgeman equation of state results. The results from both equations of state agreed well. Therefore, the ideal gas law was found to be adequate, and thus, no specific high-pressure correction was needed. The gases were injected with rapid agitation to ensure uniform mixing near the center region of the pressure vessel. Prior to injection, the hydrogen was purged through the entire feeding system before filling to ensure that any possible traces of residual nitrogen or water vapor were gone. After the purge, hydrogen was filled first, followed by high-purity air. To verify uniform mixing by the agitation method, certain tests were also conducted using an extended time period for mixing for example, 12 hr, between the gas injection and initiation of ignition. Uniform mixing by the rapid agitation method (test 11) was verified by comparing the results from test 13, which was conducted 12 hr after the gas injection. These two tests were shown to have nearly identical results, regardless of the mixing method, that is, turbulent convective mixing or normal species diffusion by concentration gradient.

High-Speed Cinematography and Video Camera Recording

In this research, flame propagation processes were observed and recorded by two techniques using a HYCAM and a Pulnix CCD camera. A semitransparent mirror was utilized so that these cameras were able to record the highly transient event through a common viewing window. The mirror was oriented at a 45-deg angle with the line sight between the HYCAM camera and the viewing window. The CCD video camera recorded the reflected image from the semitransparent mirror. The position of these two cameras can be switched as shown in Fig. 2. The semitransparent mirror reflects 45% of the incident light to the Pulnix CCD camera and transmits the remaining light (55%) to the HYCAM.

The HYCAM camera has the capability to record 44,000 pictures/s when a quarter-frame head is used. This camera instantaneously records images on 16-mm film throughout the interesting portion of the experiment. For most of the test runs, the HYCAM camera was configured to record images on 16-mm film using a half-frame head providing a framing rate of 14,000 frames/s (or 28,000 picture/s), which was adequate for capturing the details of the desired events.

The Pulnix CCD camera was used primarily as a monitoring device with instant playback. By the coupling of this high-resolution camera with a Super VHS Panasonic video cassette recorder, useful images were obtained. The Super VHS enables a recording speed of 60 frames/s. The VHS video camera's immediate feedback feature is advantageous because development and processing of the HYCAM film takes several weeks. The CCD color camera had an adjustable shutter speed that can be fixed as fast as 0.1 ms.

Flow Visualization with $TiCl_4$ Vapor

The reaction between H_2 and air is not generally visible. Illumination from the igniter was initially valuable, but later a visualization aid was needed. For some test runs, $TiCl_4$ (titanium tetrachloride) vapor was introduced into the combustor to facilitate the observation of the instantaneous flame front of the hydrogen/air mixture utilizing a pulsed copper-vapor laser sheet in conjunction with the HYCAM. Reactions between $TiCl_4$ and water vapor as one of the major combustion products from H_2/O_2 reaction form submicron TiO_2 particles that can scatter the light from the pulsed laser beam, thereby providing good spatial and temporal resolution of the flame front recorded by the HYCAM. The advancement and contours of the flame front could, therefore, be easily observed. $TiCl_4$ was injected prior to the pressurization of the chamber with the combustible mixture. The $TiCl_4$ was heated to its boiling point (136°C) to create a $TiCl_4$ vapor that was then mixed with the injected gases in the chamber. For tests using $TiCl_4$, approximately 0.2 ml of $TiCl_4$ was vaporized and diffused into the chamber prior to the injection of the combustible gases. The amount of $TiCl_4$ vapor injected is extremely small, causing no noticeable pressure increases within the combustible mixture.

To implement this system, a vapor generator was fabricated to introduce $TiCl_4$ into the chamber. The generator was constructed from an electric heating element and stainless steel tubing. The vapor generator consisted of two Swaglok fittings on each end, which made it easy to connect directly to the existing combustor ports. The vapor generator had a capacity of 7 ml of fluid. An R-type thermocouple probe was placed on the heater wall to monitor the fluid temperature. Because the boiling point of $TiCl_4$ is approximately 136°C, the heater was maintained at a temperature of 180°C during the vapor injection period to compensate for heat losses. The heater element was controlled by an ac voltage transformer, which operated on normal 120 VAC.

Data Acquisition System

The complete data acquisition system consisted of a 120-MHz Pentium personal computer, a Hewlett-Packard laser printer, and

Table 1 Summary of test conditions and results

Test no.	$X_{H2}/X_{air}/X_{CH4}$	P_I, MPa/psia	$TiCl_4$	HYCAM	Igniter type	P_{max}, MPa/psia	P_{max}/P_I	$T_{g,max}$, K
1	N_2 only	3.89/564.7	N/A	Yes	A	4.58/664.7	1.18	N/A
2	15.9/84.1/0	3.55/514.7	N/A	Yes	A	10.37/1,504.7	2.98	N/A
3	15.9/84.1/0	3.55/514.7	N/A	Yes	A	10.90/1,464.7	2.90	1600
4	15.9/84.1/0	3.55/514.7	N/A	Yes	A	6.24/904.7	1.78	1100
5	15.9/84.1/0	3.55/514.7	N/A	Yes	A	7.06/1,024.7	2.02	1250
6[a]	11.0/87.0/2	3.45/500	N/A	Yes	A	4.29/622.7	1.25	1300
7	13.0/87.0/0	3.45/500	N/A	N/A	A	4.24/614.7	1.24	540
8	13.0/87.0/0	6.89/1,000	N/A	Yes	B	9.65/1,399.7	1.41	975
9	13.0/87.0/0	6.89/1,000	Yes	Yes	B	7.38/1,069.7	1.07	820
10	13.0/87.0/0	13.79/2,000	N/A	Yes	B	15.17/2,199.7	1.10	1600
11	13.0/87.0/0	20.68/3,000	N/A	Yes	B	21.82/3,164.7	1.06	1280
12	13.0/87.0/0	20.68/3,000	Yes	Yes	B	21.47/3,114.7	1.04	450
13	13.0/87.0/0	18.37/2,665	N/A	Yes	B	19.87/2,882.2	1.08	750
14	13.0/87.0/0	20.68/3,000	N/A	N/A	B	21.92/3,180	1.06	525
15	13.0/87.0/0	20.68/3,000	——	——	B, failed	——	——	——
16	13.0/87.0/0	20.68/3,000	N/A	N/A	B	22.22/3,223	1.07	1283
17	15.9/84.1/0	3.55/514.7	N/A	N/A	B	10.78/1,563.4	3.10	N/A
18	15.9/84.1/0	20.68/3,000	N/A	N/A	B	39.26/5,694	1.90	N/A
19	14.0/86.0/0	20.68/3,000	N/A	N/A	B	23.5/3,408.4	1.14	N/A
20	15.0/85.0/0	20.68/3,000	N/A	N/A	B	23.34/3,819.7	1.27	N/A
21	15.9/84.1/0	20/2,900	N/A	N/A	B	32.17/4,665.2	1.61	N/A
22	15.0/85.0/0	20.68/3,000	Yes	Yes	B	36.85/5,345.2	1.79	1450

[a]Test of methane- (CH_4-) containing mixture is limited to produce clean-burning products.

a Nicolet Multipro system. The state-of-the-art Nicolet Multipro has the capability of utilizing six 120 boards for data acquisition. It has variable sampling rates that can reach a maximum sampling rate of up to 1 MHz. Each board contains four channels to record data (a 24-channel total capacity). The boards are driven with an internal clock or by an external Transistor-Transistor Logic clock signal. Each board can be triggered automatically or manually, by an external device. The Multipro has 1 Mbyte of memory per board, which is divided equally to each activated channel on the board. The system also has 12-bit resolution and full-scale inputs (from 30 mV to 12 VDC or 30 mV to 120 VAC). Because the system is equipped with differential voltage inputs, each channel has the ability to accept ac, dc-ground, and dc-to-dc connections.

The settings for this multichannel recorder were nearly the same throughout the test series in this investigation. The sampling rate was 6.25 kHz and the data sweep time was approximately 10.5 s. Four out of the possible six boards were used to acquire data in this research. The first board recorded the four thermocouple signals. The second board was used for triggering a reference point in time. The third board was programmed to record the chamber's pressure transducers. The remaining two pressure transducers in the exhaust port were recorded in the fourth board.

Discussion of Results

Typical Results

A series of tests was conducted at various initial chamber pressures and gas mixture concentrations. To simulate HGI inflator performance in the windowed high-pressure chamber, a series of intermediate steps was required to adjust and validate the test method. Table 1 summarizes the test matrix of the initial conditions and also serves to tabulate summary results. The difference in gas composition of various mixtures depends on the prescribed hydrogen mole fraction. In the course of these investigations, hydrogen mole fraction ranged from 13 to 15.9%, initial chamber pressure P_I varied from 3.45 to 20.68 MPa (from 500 to 3000 psia), and two variations of the TRW igniter assemblies were used. The igniter assembly (shown in Fig. 4) referred to as type B gives a slightly stronger pressure pulse than type A, though these two igniters have nearly identical geometric shapes. Another difference is that the igniter cap of the type A igniter is typically ejected in the vertical direction. The igniter cap of the type B igniter is usually ejected at an oblique angle. However, type A igniters produce large maximum pressure P_{max} deviations in comparison with the type B igniters.

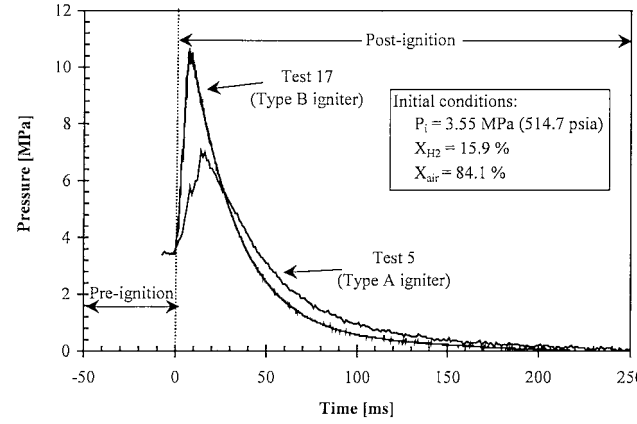

Fig. 4 Comparison of *P–t* traces from two test runs conducted under the same initial conditions using different igniters.

The initial chamber temperature for all test runs was 298 K. The initial premixed gas temperature in the combustor simulator was approximately 298 K. Table 1 has a summary of the text matrix containing the initial conditions and summarized final results of each individual experiment.

Tests 1–10 (plus test 17), at lower initial fill pressures P_I provided preliminary information and served to check methods. Tests 11–22 (excluding test 17) at $P_I = 20$ MPa (3000 psia) are of practical interest. As an example, test 4 is representative. The system was filled to 3.55 MPa at X_{H2}/X_{air} mole fractions of 15.9/84.1%. Ignition produced HYCAM images as shown in Figs. 5a and 5b, which only spans 1.6 ms of the event. The flame front leaves the field of view through the 95-mm (3.75-in.) window by approximately 0.7 ms. At that rate, the front would reach the opposite end of the chamber at 1.7 ms. Note from the *P–t* data of test 5 (very similar to test 4) and test 17 in Fig. 5 that pressure has risen in the chamber to only 3.68 MPa (534.4 psia) at 0.7 ms, indicating much of the energy remains to be released. Pressure in the vessel in fact does not peak until 16 ms.

Because rupture of the pressure seal is coincident with the igniter function, gas begins to flow out of the igniter inflator assembly within a few milliseconds of the firing signal. The rising dP/dt represents the significant effect of the heat release within the reacting mixture, which outpaces the competing process, mass flowing out

of the combustion chamber system until they balance, followed by blow down of the remaining gases.

Pressure Measurements

Shown earlier in Fig. 4 is a comparison of pressure–time traces for two test runs conducted under identical initial conditions [$P_I = 3.55$ MPa (514.7 psia) and $X_{H2} = 15.9\%$]. The tailorability is evident even at these low initial chamber pressures. Test 5 utilized the type A igniter and test 17 used the type B igniter. Pressure rise in the vessel after ignition was doubled, indicating the strong effect of igniter strength on P_{max}. P_{max} for all other tests is tabulated in Table 1. The pressure peak duration can be defined as the time elapsed for the pressure to return to the initial chamber pressure. It is obvious that the igniter strength can not only influence P_{max}, but the entire pressure–time history. For test 5, 50 ms elapsed before the pressure returned to 20.68 MPa (3000 psia). However, it only took 40 ms for test 17 to return to the original pressure. By comparing the results of tests 2–5, it is noticeable that the strength variability of the igniter can also affect the magnitude of the pressure pulse in a nonnegligible fashion.

Observation by High-Speed Cinematography

Individual frames selected from the high-speed movie film of test 4 (utilizing the type A igniter) are shown in Figs. 5a and 5b. Detailed film interpretations are given adjacent to each photograph. Note that the photographs indicate propagation from right to left; however, the orientation of propagation in the windowed high-pressure strand burner was from the bottom to the top. The igniter produced a flame front that was generally one-dimensional during its propagation. In other words, the observed HYCAM images of the flame front tended to form a nearly planar luminous front and remain generally uniform during its propagation through the observable 95 mm (3.75 in.). The major reason for uniform flame-front propagation is that the ejected igniter cap traveled along the longitudinal axis of the combustor. The igniter cap trajectory also seemed to control the flame propagation speed. The base of the ascending igniter cap served as the flame holder due to the existence of the recirculating wake region behind its base. These uniform features were consistently observed for the propagating flame front in tests 2–7, each using type A igniter assemblies. For these test runs, the igniter cap traveled upward and appeared to be seated at the flame front.

In general, when the burned gas began to discharge from the combustor toward the annular igniter exit port, the flame continued to propagate upward (out of view), as shown in Fig. 5b. Later, the overall luminous region diminished quickly, particularly near the top region of the combustor. The luminosity in the lower portion of the combustor (right side of the viewing port) was still supported by the continued igniter discharge. Deposits of water droplets condensed on the viewing port became visible in the later photographs as fixed white spots (pictures 16–28). This 10-picture series only represents the 40% of recorded film images from the field of view. The remaining segment in the combustor was largely invisible by the HYCAM movie film without illumination techniques such as the laser sheet/$TiCl_4$ vapor.

A series of selected pictures from the high-speed movie film of test 12 (utilizing type B igniter) is shown in Figs. 6a and 6b. Again, detailed film interpretations are given adjacent to each photograph. As already stated, the igniter cap trajectory of the type B igniters are quite different from that of the type A igniters. Figure 6a shows that although the cap of the igniter rides on the flame front, the igniter cap trajectory angle (relative to the longitudinal axis) is much greater than 0 deg. After approximately 0.286 ms (not shown in Figs. 6), the cap begins to become canted to the bottom of the photograph (actually to the left of the chamber). The same flame-holding phenomenon also exists in this series of photographs. Once again, it appears that the base of the cap forms a flame holder. However, it also was tumbling slowly and drifting toward the vessel wall. The last four pictures in Fig. 6b show the existence of many bright particles moving slowly along the window surface. These bright

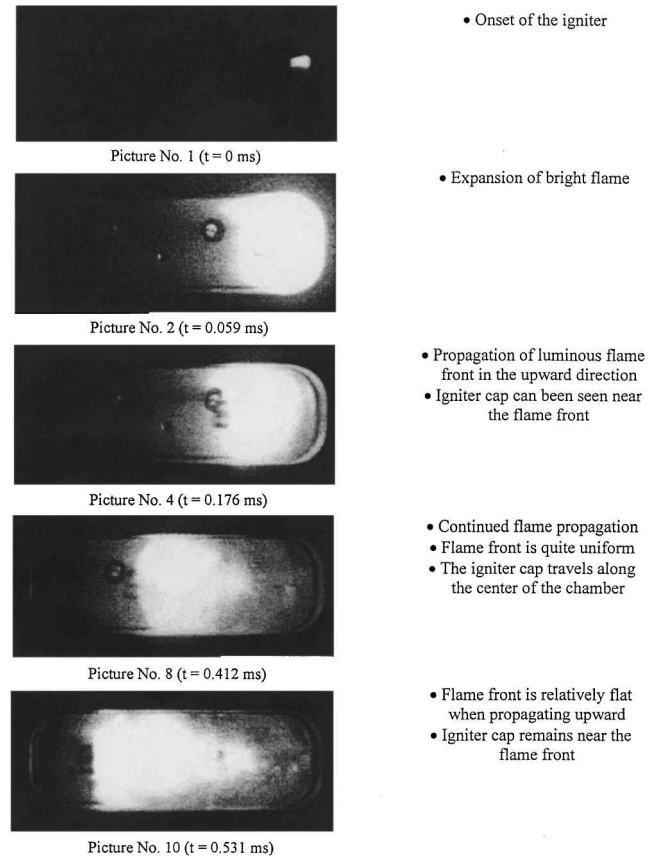

Fig. 5a Set of selected pictures from HYCAM film of test 4 with H_2/air (15.9/84.1), t = 0–0.531 ms.

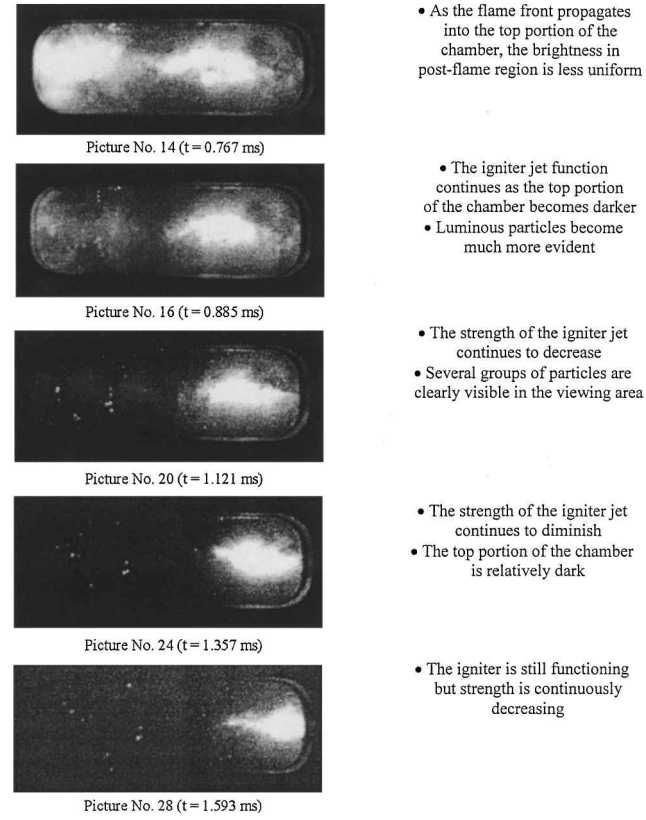

Fig. 5b Pictures from HYCAM film of test 4 with H_2/air (15.9/84.1), t = 0.767–1.593 ms.

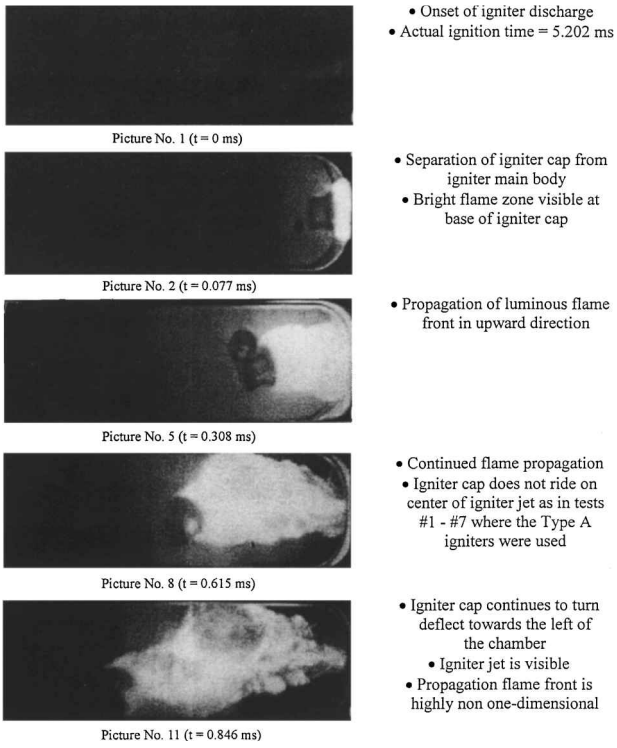

Fig. 6a Set of selected pictures from HYCAM film of test 12 with H_2/air (13/87), t = 0–0.846 ms.

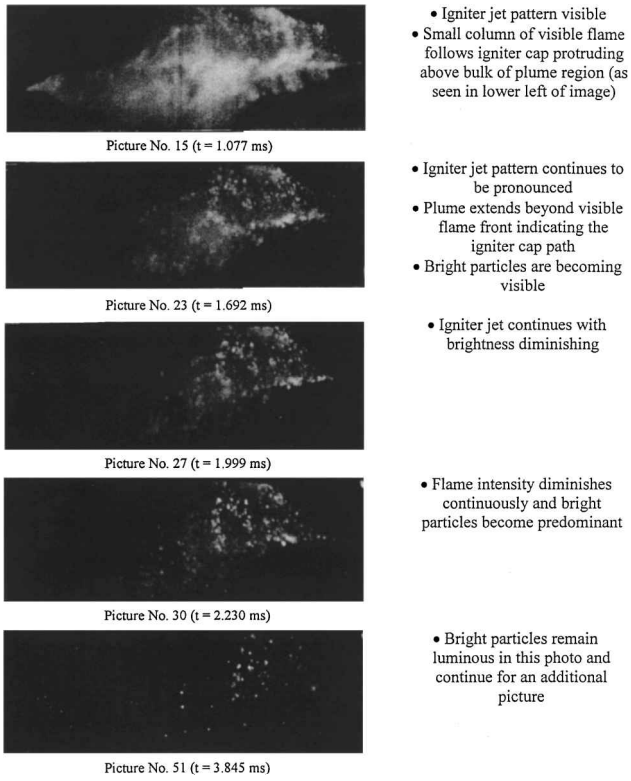

Fig. 6b Pictures from HYCAM film of test 12 with H_2/air (13/87), t = 1.077–3.845 ms.

particles are believed to be water droplets that condensed on the window surface.

The particle number density of test 12 is higher than that of test 4 (shown in Fig. 5b). This phenomenon is believed to be caused by two factors: increased chamber pressure is higher [P_I = 20.68 MPa (3000 psia) for test 12 vs P_I = 3.55 MPa (514.7 psia)] and a higher heat transfer rate between the window and the flame front, resulting in a greater possibility of condensation. The canted

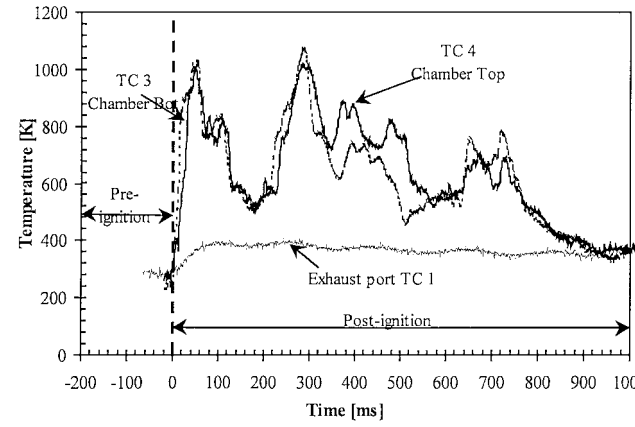

Fig. 7 Measured temperature–time traces from the combustor and exhaust line test 4.

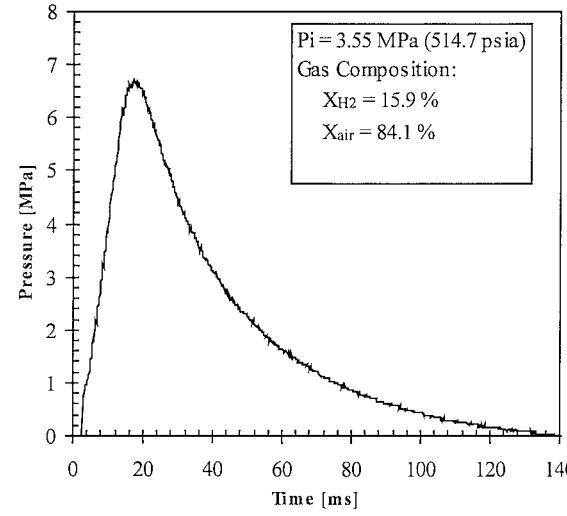

Fig. 8 Measured exhaust port pressure–time trace from test 17.

flame-front trajectory can also produce stronger interaction between the combustion product gases and the cold window surface.

Temperature Measurements

Figure 7 shows the measured temperature–time traces from test 4. The burned-gas temperature near the diagnostic window replacement plate (6 and 25 mm from the chamber wall) was measured by two S-type fine-wire thermocouples (TCs) (TC 3 and TC 4, respectively). These two traces were quite similar, even though the distance between the junction beads was approximately 50 mm (2 in.). This implies that the turbulent eddies were significantly large for production of a coherent eddy structure. Temperature measurements, shown in Fig. 7, show the rise to 1000 K in the gas at TC 3 precedes that of TC 4, reflecting its position 50 mm closer to the igniter. TC response, of course, lags the transient event, but is nevertheless useful information.

The 10 selected photographs in Fig. 5a correspond to the initial temperature rise; thereafter, the combustion process was very dark. The distinct time variations of the TC outputs are believed to be caused by the intermittent engulfment of the TC junctions in the turbulent flame boundary. These TC traces indicate the occurrence of substantial combustion events after the visible time period. TC 1, located in the exhaust line, exhibited a nearly constant temperature (around 400 K) for a relatively long period time. This low temperature indicates the adequacy of the exhaust gas temperature for airbag inflation.

Exhaust Port Pressure Measurements

The exhaust port pressure–time trace for test 17 (under identical test conditions as test 4) is shown in Fig. 8. Because in this experiment the product gas was exhausted through the annular HGI

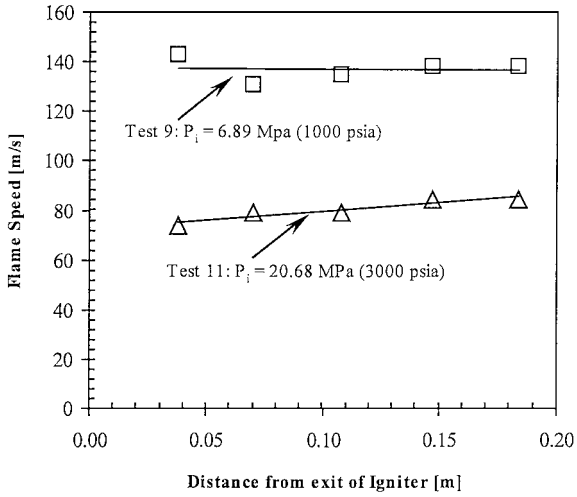

Fig. 9 Comparison of two typical flame propagation speed profiles.

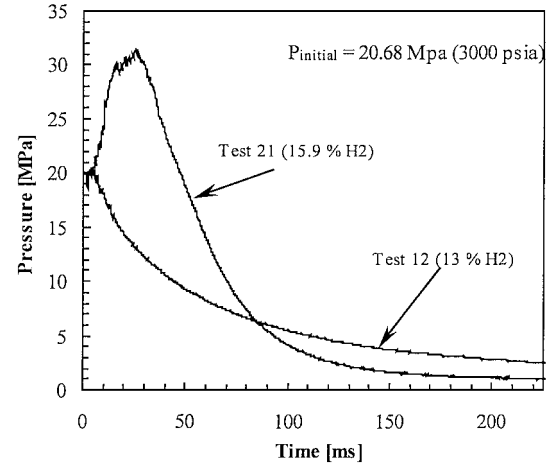

Fig. 10 Comparison of recorded pressure–time traces from two test runs with different initial H_2 mole fractions.

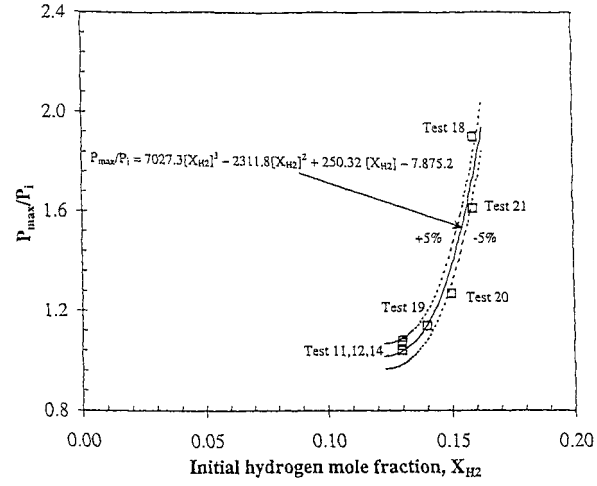

Fig. 11 Dependence of initial H_2 mole fraction on peak pressure.

igniter port and the base plate to the ambient atmosphere, this measured pressure–time trace is somewhat different from TRW's published data.[3] In previous work at TRW, the product gases were exhausted to a 146-liter ballistic tank maintained at room temperature.[3] This tank was used to simulate the filling process of an airbag for a midsize vehicle. Note from this pressure–time trace that the effective time for bag inflation is around 40 ms.

Effect of Initial Chamber Pressure on Flame Propagation Speed

The deduced flame propagation speeds from HYCAM movie films appear to be nearly constant for most of the test runs. Figure 9 shows typical results of two deduced flame speed variations as the flame propagates from right to left in the visible window region. For test 9, with an initial chamber pressure of 6.89 MPa (1000 psia), the average flame propagation speed was around 137 m/s, which is substantially higher than that of test 11 conducted at 20.68 MPa (3000 psia). At higher pressures, the speed of the igniter cap was reduced due to the increased drag force. The constancy of the flame propagation speed is believed to be associated with the uniformity of the premixed reactive gases as well as the weak wall-cooling effect during the initial flame propagation interval. Typical flame speeds are as follows: 1) low-pressure tests [<6.89 MPa (1000 psia)], $V_{\text{flame}} = 135$–155 m/s and 2) high-pressure tests [= 20.68 MPa (3000 psia)], $V_{\text{flame}} = 75$–85 m/s.

Hydrogen Mole Fraction and Pressure Effects

Even though the final peak chamber pressure seemed to have a dependence on both the initial hydrogen mole fraction and the initial chamber pressure, it was found that the initial hydrogen mole fraction had the greatest impact on the pressurization rate of all test runs. Figure 10 shows a direct comparison of two tests conducted under the identical initial chamber pressure of 20.68 MPa (3000 psia), but with different initial hydrogen mole fractions, 13 and 15.9%, respectively. The pressure–time profile for test 21 ($X_{H2} = 15.9\%$) exhibits a significant pressure increase shortly after ignition. The maximum pressure was 1.61 times higher than the initial chamber pressure; this condition is desirable for airbag inflation purposes. In test 12 ($X_{H2} = 13\%$), the pressure rise is almost insignificant. The maximum pressure to initial pressure ratio only reached 1.04. Besides the $P_{\max}/P_I$ ratio, the entire pressure–time history of the test runs was significantly affected by the initial H_2 mole fraction, as evidently shown in Fig. 10.

In Fig. 11, the pressure ratio $P_{\max}/P_I$ is displayed as a function of initial hydrogen mole fraction for tests conducted at the initial pressures around 20.68 MPa (3000 psia) using the type B igniters. It is obvious that the initial hydrogen mole fraction is extremely sensitive. A second-order polynomial curve fit was developed to relate these two parameters. In general, the pressure ratio drastically increases as the mole fraction of hydrogen increases. Note that when the system was operated under very fuel-lean conditions, that is, $X_{H2} \sim 13\%$, the pressure ratio of $P_{\max}/P_I$ is close to unity, and any pressure rise is believed to be governed by the discharge pulse of the igniter. The combustion process under such a fuel-lean condition is very marginal and depends on the interaction between the igniter and the premixed gases. When the trajectory of the igniter cap is highly canted, the igniter discharge jet will interact with a smaller amount of premixed reactive gases. If the trajectory angle of the igniter cap is very close to 0 deg, the wake region generated by the ejected cap has a greater possibility to entrain a larger amount of premixed gases for reaction. Therefore, it is expected to have poor reproducibility in pressure–time traces for very lean mixtures.

This concept is verified in Fig. 12, which exhibits a comparison of two tests conducted under identical initial fuel-lean conditions ($X_{H2} = 13\%$), using the same B-type igniter. Figure 12 shows that the appearance of the second pressure peak was occurring at significantly different times. The magnitudes of these second pressure peaks are also very different even though these two traces overlapped for a short initial period. For test 16, the second pressure peak was very noticeable early in the test run. For test 11, the second pressure peak was observed at a much later time, during the depressurization process. The reason for the early occurrence of the second pressure peak in test 16 is believed to be a result of a better trajectory angle of the ejected igniter cap. In the case of test 11, the ejected igniter cap trajectory had a large oblique angle so that the wake region behind the cap did not entrain a large amount of premixed gas. As a result, residual premixed gases (fuel and oxidizer) were burned at a much later time than desired.

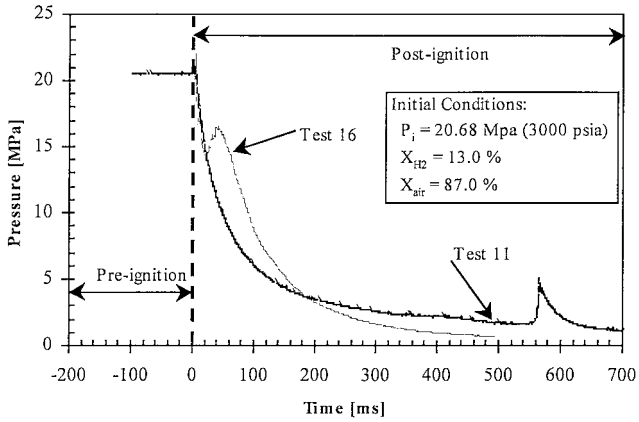

Fig. 12 Pressure–time trace reproducibility under fuel-lean test conditions.

To improve the reproducibility of the pressure–time traces during the depressurization interval, it is suggested to avoid extremely fuel-lean situations. It is also beneficial to use highly reproducible igniters for this purpose.

Conclusions

Several major conclusions are summarized as follows.

1) The flame-front propagation process in the HGI combustor is governed by the trajectory of the ejected cap of the igniter.

2) For type A igniters, the igniter action time is approximately 1.8 ms. The igniter cap was ejected mostly in the upward direction; the flame front of the reacting mixture was quite uniform. For type B igniters, the igniter cap was generally ejected at an oblique angle; therefore, the flame front was non-one-dimensional

3) The flame propagation speed for tests that had an initial chamber pressure of 6.89 MPa (1000 psia) and 20.68 MPa (3000 psia) were 135–155 m/s and 75–85 m/s, respectively. At higher initial chamber pressures the drag force on the igniter cap is increased, which reduced the flame propagation speed.

4) The short flame propagation event was captured and recorded using high-speed cinematography. The duration of observing visible flame images is much shorter than the overall transient event. The major combustion interval of H_2/air mixture during the depressurization process in not luminous. However, TC traces indicated the occurrence of exothermic reactions. The similarity of the TC traces that were measured at a large distance apart suggest the production of large coherent eddy structures in the flame zone. The measured gas temperature in the exhaust line was nearly constant (around 400 K) for a relatively long period of time.

5) The initial mole fraction of hydrogen was found to have a pronounced effect on the pressure–time history in the combustor. The pressure–time traces for very fuel-lean mixtures ($X_{H2} = 13\%$) are highly nonreproducible with a second pressure peak appearing at a random time interval. This randomness is believed to be associated with the nonreproducibility of the igniter cap ejection trajectory. Therefore, it is suggested to avoid the use of very lean-gas mixtures for improving the reproducibility of the HGI bag filling process.

References

[1]Sherman, D., "The Rough Road to Airbags," *Invention and Technology*, Summer Issue, 1995, pp. 48–56.

[2]Scheffee, R. S., "Gas Generating Composition with Polyvinyl Chloride Binder," U.S. Patent filed 7 May 1971, Serial No. 141,311. Int. Cl. C06d 5/06; patented 3,723,205, 27 March 1973.

[3]Stansel, J. C., and Blumenthal, J. L., "Heated Gas Inflator Technology," *Proceedings of the 2nd International Symposium on Sophisticated Car Occupant Safety Systems: Air Bag 2000 Conference*, Fraunhofer-Institut Für Chemische Technologie, Karlsruhe, Germany, 1994, pp. 12-1–12-10.

[4]Blomquist, H., Green, P., Freesmeier, J., Butler, B., and Krier, H., "Modeling Heated-Gas Airbag Inflators," *Proceedings of the 2nd International Symposium on Sophisticated Car Occupant Safety Systems: Air Bag 2000 Conference*, Fraunhofer-Institut Für Chemische Technologie, Karlsruhe, Germany, 1994.

[5]Faerber, E., "Benefits of Fitting Airbags to Passenger Cars," *Proceedings of the 2nd International Symposium on Sophisticated Car Occupant Safety Systems: Air Bag 2000 Conference*, Fraunhofer-Institut Für Chemische Technologie, Karlsruhe, Germany, 1994, p. 14-1.

[6]Deppert, T. M., Barnes, M. W., Mendenhall, I. V., and Taylor, R. D., "Development of Gas Generants for Passive Automobile Restraint Systems," *Proceedings of the 2nd International Symposium on Sophisticated Car Occupant Safety Systems: Air Bag 2000 Conference*, Fraunhofer-Institut Für Chemische Technologie, Karlsruhe, Germany, 1994, pp. 10-1–10-17.

[7]Khandhadia, P., Klosinski, R., and Vitek, J., "Advanced Inflator Technology for Automotive Airbag," *Proceedings of the 2nd International Symposium on Sophisticated Car Occupant Safety Systems: Air Bag 2000 Conference*, Fraunhofer-Institut Für Chemische Technologie, Karlsruhe, Germany, 1994, pp. 11-1–5-16.

[8]Ericsson, D., Sanden, R., and Tryman, R., "A Comparative Study of Some Energetic Air-Bag Compositions Concerning Toxic Combustion Products," *Proceedings of the 2nd International Symposium on Sophisticated Car Occupant Safety Systems: Air Bag 2000 Conference*, Fraunhofer-Institut Für Chemische Technologie, Karlsruhe, Germany, 1994, pp. 36-1–36-9.